AD NUMBER

AD843084

NEW LIMITATION CHANGE

TO

Approved for public release, distribution unlimited

FROM

Distribution authorized to U.S. Gov't. agencies and their contractors; Critical Technology; 01 OCT 1968. Other requests shall be referred to Air Force Rocket Propulsion Laboratory, Attn: RPPR-STINFO, Research and Technology Division, Edwards AFB, CA.

AUTHORITY

afrpl ltr, 27 oct 1971

AFRPL-TR-68-164

CARBIDES FOR SOLID PROPELLANT NOZZLE SYSTEMS

F. T. LALLY
D. P. LAVERTY
TRW Inc.

TECHNICAL REPORT AFRPL-TR-68-164
1 OCTOBER 1968

 attn: RPPR-STINFO

AIR FORCE ROCKET PROPULSION LABORATORY
RESEARCH AND TECHNOLOGY DIVISION
EDWARDS, CALIFORNIA 93523
AIR FORCE SYSTEMS COMMAND, UNITED STATES AIR FORCE

43

NOTICES

When Government drawings specifications, or other data are used for any purpose other than in connection with a definitely related Government procurement operation, the United States Government thereby incurs no responsibility nor any obligation whatsoever; and the fact that the Government may have formulated, furnished or in any way supplied the said drawings, specifications, or other data, is not to be regarded by implication or otherwise as in any manner licensing the holder or any other person or corporation, or conveying any rights or permission to manufacture, use, or sell any patented invention that may in any way be related thereto.

Qualified requesters may obtain copies from DDC, Document Service Center, Cameron Station, Alexandria, Virginia 22314. Orders will be expedited if placed through the Librarian or other persons designated to request documents from DDC.

DDC release to CFSTI is **NOT** authorized because the report contains technology identifiable with items on the strategic embargo lists excluded from export or re-export under the U.S. Export Control Act of 1949 (63 STAT. 7), as amended (50 U.S.C. App. 2020-2031), as implemented by AFR 400-10, AFR 310-2, and AFSCR 80-20.

Copies of this report should not be returned unless return is required by security considerations, contractural obligations, or notice on a specific document.

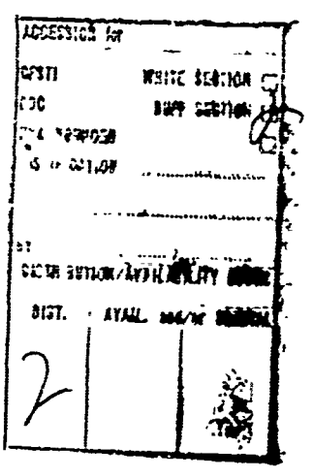

CARBIDES FOR SOLID PROPELLANT NOZZLE SYSTEMS

F. T. Lally
D. P. Laverty

FOREWORD

This report is the final technical report summarizing the results of the work performed under Contract FO 4611-67-C-0094 covering the period of 1 October 1967 to 30 June 1968. The progress made during the final month of the program (1 June 1968 to 30 June 1968) is also included in this report. This report has been assigned the TRW internal Report Number ER 7307.

This contract with TRW Incorporated, Cleveland, Ohio was sponsored by:

Air Force Rocket Propulsion Laboratory

Research and Technology Division

Edwards, California

Air Force Systems Command

United States Air Force

Lt. David Zorich acted as Project Engineer.

This technical report has been reviewed and is approved.

Lt. David Zorich
Project Engineer
Air Force Rocket Propulsion Laboratory

ABSTRACT

The magnitude of reactivity between Al_2O_3 and carbide composite rocket nozzle throat materials was assessed by means of laboratory tests. A secondary objective of the program was to establish the validity of the laboratory tests in evaluating material performance. The program included a plasma jet test that measured mechanical and chemical erosion and a static reactivity test to separate the purely chemical effects. A prediction of the performance of the carbide composites in a test firing was made, based on the laboratory tests.

TABLE OF CONTENTS

	Page
INTRODUCTION	1
MATERIALS AND TEST PROCEDURE	2
Material	2
Test Procedure	2
Plasma jet impingement tests	2
Static reactivity tests	
Specimen evaluation	4
TESTS RESULTS	5
Microcomposites	5
Jet impingement	5
Static reactivity	5
Hypereutectic Carbides	12
Jet impingement	12
Static reactivity	12
Metallurgical Analysis of Specimens	17
Metallography	17
Electron microprobe	22
X-ray diffraction	28
DISCUSSION OF RESULTS	30
Microcomposites	30
Hypereutectic	31
CONCLUSIONS AND PREDICTION OF FIRING BEHAVIOR	32

LIST OF ILLUSTRATIONS

Figure		Page
1	Schematic Diagram of Plasma Jet Impingement Apparatus	3
2	Appearance of 8Ta-55Hf-37C Microcomposites After Exposure to Al_2O_3 Seeded Plasma Jet Tests	6
3	Appearance of 8Ta-54Hf-38C Microcomposites After Exposure to Al_2O_3 Seeded Plasma Jet Tests	7
4	Erosion Rates of Ta-Hf-C Microcomposites Compared to Various Nozzle Materials, Plasma Jet Impingement Tests, Alumina Seeded, 0.5 lbs/hr.	9
5	Appearance of 8Ta-54Hf-38C Microcomposites After Exposure to Al_2O_3 in the Static Reactivity Tests	11
6	Appearance of the 3rd Group of Carbide Composites After Exposure to Al_2O_3 Seeded Plasma Jet Tests	14
7	Appearance of the 4th Group of Carbide Composites After Exposure to Al_2O_3 Seeded Plasma Jet Tests	15
8	Erosion Rates of Hypereutectic TaC-C Carbides Compared to Various Nozzle Materials During Impingement with a Plasma Jet Seeded with Alumina at 0.5 lbs/hr.	16
9	Microstructure of the As-Received Microcomposite	19
10	Microcomposite Material After the Alumina Seeded Plasma Jet Test at 5600°F	19
11	Microstructure of the 8Ta-54Hf-38C Microcomposite After a 3 Minute Exposure at 4600°F in Contact with Al_2O_3	20
12	Microstructure of As-Received TaC-C Hypereutectic Composite. Aerojet Specimen No. 462 J	21
13	Hypereutectic TaC-C Composites After the Al_2O_3 Seeded Plasma Jet Tests	22

LIST OF ILLUSTRATIONS

Figure		Page
14	Electron Microprobe Photographs of the Microcomposite Material After the Alumina Seeded Plasma Jet Test at 5600°F	24
15	Electron Microprobe Photographs of the 8Ta-54Hf-38C Microcomposite After Static Reactivity Testing at 4600°F in Contact with Al_2O_3	25
16	Electron Microprobe Photographs of the 8Ta-54Hf-38C Microcomposites After Static Reactivity Testing at 5100°F in Contact with Al_2O_3	26
17	Electron Microprobe Photographs of the Reacted Zone within the TaC-C Composite, Specimen 463b - Table 3, After the Alumina Seeded Plasma Jet Test at 4650°F	27
18	Electron Microprobe Photographs of the Area within the Build Up Reaction Product of the TaC-C Composite Specimen 463b - Table 3, After the Alumina Seeded Plasma Jet Test at 4650°F	28
19	Electron Microprobe Photographs of the TaC-C Composite (Specimen No 488-2 - Table 4), After Static Reactivity Testing at 4750°F	30

LIST OF TABLES

Table		Page
1	Plasma Jet Impingement Data, Al_2O_3 Seeded	8
2	Test Conditions for the Alumina-Microcomposite Carbide Static Reactivity Tests	10
3	Plasma Jet Impingement Data, Al_2O_3 Seeded 3rd Group of Carbide Composites	13
4	Static Reactivity (Sessile Drop) Test - Al_2O_3 3rd Group of Carbide Composites	17

INTRODUCTION

The performance of rocket nozzle inserts with relatively small throat diameters is often dependent upon maintaining the dimensional integrity of the nozzle throat section during the firing cycle. The primary degradation mechanisms involve melting, thermal shock, and the combined effect of chemical reactivity and mechanical erosion. Recent work has indicated that carbides are susceptable to surface degradation by chemical reactivity when exposed to alumina (Al_2O_3) at temperatures substantially below the carbide melting points. As a result, the limiting consideration in selecting the high melting carbides for Aluminum containing solid propellant rocket nozzle application may be chemical reactivity rather than melting point.

Due to the complexity of the degradation mechanisms operating in the nozzle throat during the firing cycle, it is desirable to isolate the effects of the individual mechanisms by a laboratory test. The subject program was aimed at establishing the magnitude of the reactivity problem between Al_2O_3 and carbide composites being considered for rocket nozzle throat materials. A secondary objective of the program was to establish the validity of the laboratory tests as a tool for evaluating nozzle throat material performance potential.

The program included a plasma-jet test that subjected the specimen to high temperatures and impingement of Al_2O_3 particles to measure the combined effects of mechanical erosion and chemical erosion. The effect of chemical reactivity alone was evaluated by a static reactivity (sessile drop) test wherein the selected composite material was heated to 4500°F or higher in contact with molten Al_2O_3.

MATERIALS AND TEST PROCEDURE

Test Material

The material evaluated during this program consisted of four distinct carbide composites furnished by the Government. The first and second sets of materials were Ta-Hf-C microcomposites produced by the Aerojet-General Corporation by hot pressing. The materials are described in report Nos. AFRPL-TR-66-282, AFRPL-TR-67-13, and AFRPL-TR-67-207. The chemical composition of these materials were identified by Aerojet-General as 8Ta-55Hf-37C and 8Ta-54Hf-38C.

The third and fourth sets of carbide materials tested in this program were also received from Aerojet-General Corporation. These specimens, which were not identified as to specific composition, are hypereutectic TaC-graphite composites produced by fusion casting and containing varying percentages of graphite. The fourth carbide composite which was to be TaC clad and hence tested in the unmachined condition. The samples were tested with the square cross section as furnished by Aerojet. All other specimens were machined to a 0.250 inch diameter prior to testing.

Test Procedure

Plasma-jet impingement tests - The apparatus for conducting the plasma-jet impingement tests is shown in the schematic diagram of Figure 1. The specimen, a 1/4 inch diameter x 2 inch long rod is resistance heated by 220V powerstats which are capable of developing temperatures up to 6000°F. The plasma-jet is attached to a movable arm which allows the gun to be rotated into the plane of the specimen. The erosion resistance is measured as a function of temperature by maintaining a fixed gun distance and independently varying the temperature of the resistance heating (preheat). An argon environment was used in the chamber with an alumina injection rate of 0.5lbs./hr. and a heat flux from the gun of approximately 1200 BTU/ft^2-sec. Temperatures were measured during the test with an optical pyrometer. The test duration was three minutes and the change in diameter was used as the evaluation parameter.

Static reactivity tests - The static reactivity was measured by sessile drop tests which were carried out with a 1/4 inch diameter rod type specimen heated by resistance to the desired temperature. A cavity, machined in the top of the specimen, was filled with Al_2O_3 powder. The specimen had the least cross section at the bottom of the cavity and therefore reached its highest temperature in this area. These tests were carried out for a duration of 3 minutes in an atmosphere of flowing argon.

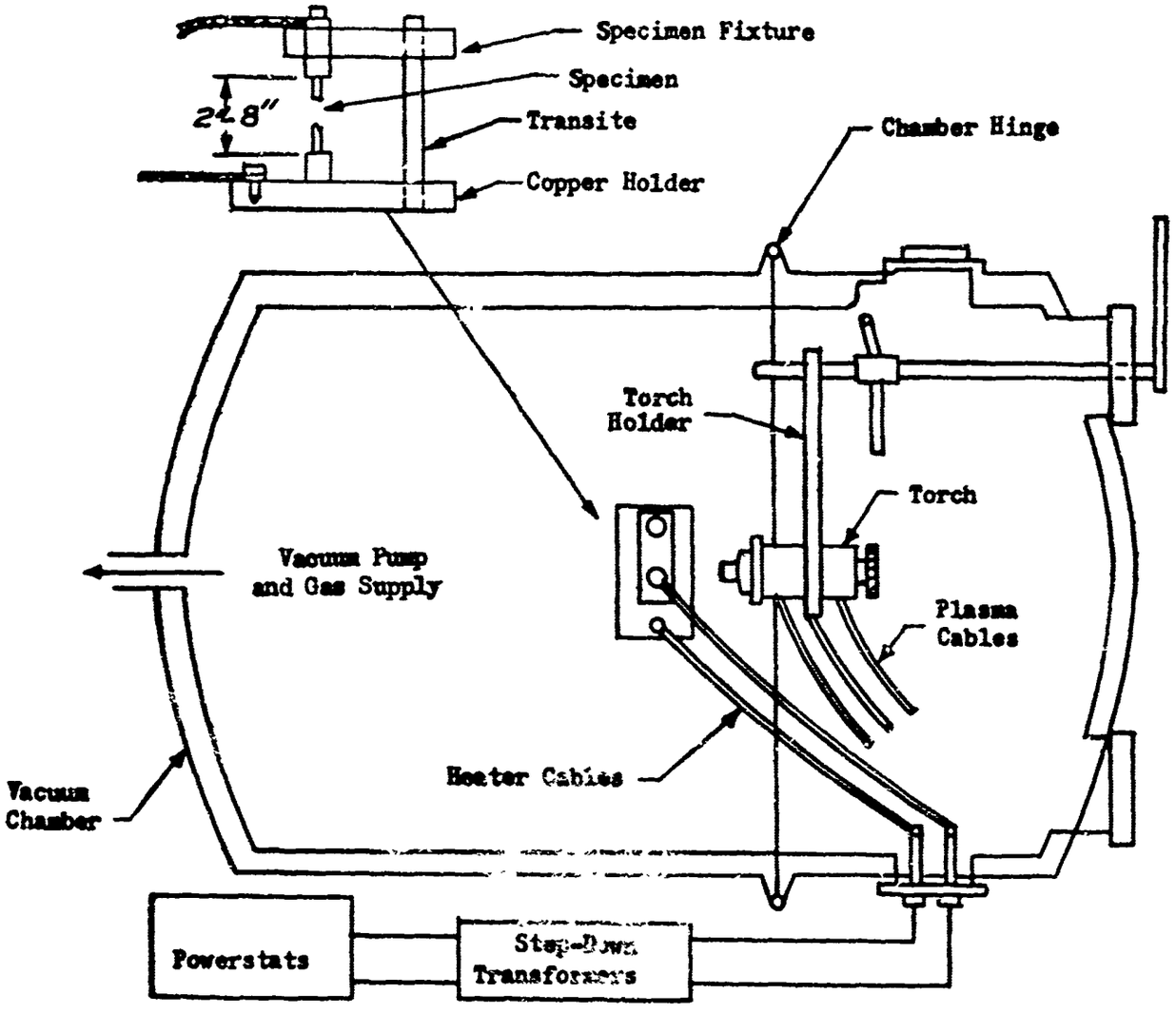

Figure 1. Schematic Diagram of Plasma Jet Impingement Test Apparatus

Specimen evaluation - The main evaluation criterion in these tests was the depth of surface reactivity or erosion experienced by the specimen during the test. In addition to erosion measurements, the specimens were evaluated by metallographic examination, electron microprobe, and x-ray diffraction to assess the nature and extent of chemical reactions and to define the mechanisms of attack.

TEST RESULTS

The results of both the plasma jet impingement tests and the static reactivity tests on the two sets of microcomposites materials will be presented first, since these two sets of specimens behaved similarly to each other. The results obtained on the hypereutectic carbides will then be presented so that an overall comparison of the various materials can be made.

Microcomposites

Plasma jet impingement tests - The first specimen of the 8Ta-55Hf-37C composition was brought up to a preheat temperature of 4250°F by resistance heating in approximately 15 seconds. The specimen failed catastrophically (apparently by melting) before the plasma gun could be rotated into place. Specimen No. 2 was then preheated at a much slower rate, requiring 18 minutes to reach 5600°F, and then cooled to room temperature. This specimen failed during the cool-down cycle due to mechanical stresses imposed by the clamping mechanism. All remaining specimens that required preheating were brought up to temperature at a rate of 1000°F per minute. The appearance of the 8Ta-54Hf-37C microcomposite specimens after testing are presented in Figure 2; the 8Ta-55Hf-38C material is shown in Figure 3.

The data derived from the plasma-jet impingement tests of both microcomposites materials are tabulated in Table I. The erosion rate is also plotted as a function of test temperature in Figure 4. The erosion rates of other refractory nozzle materials are included in the graph of Figure 4 for comparison.

In general, the erosion resistance of both of the microcomposites materials in the alumina seeded plasma jet tests is comparable to that of stoichiometric HfC at temperatures of 5400°F and higher. Below this temperature, the data indicated a somewhat lower erosion rate for the microcomposite materials. The results also indicated that, in common with the stoichiometric HfC, a threshold temperature between 5400-5600°F exists above which the recession rate increases rapidly.

Static reactivity of microcomposites The conditions of the static reactivity tests of the microcomposites materials are tabulated in Table 2. (The disposition of the 20 microcomposite specimens received from the Government is also included in Table 2.)

The specimens, after testing, are shown in Figure 5. The fracture of specimen No. 3 occurred after 2.2 minutes at 4800°F and was accompanied by severe evidence of deformation of the specimen. All specimens in this test showed some evidence of deformation, although not as severe as that of specimen No. 3.

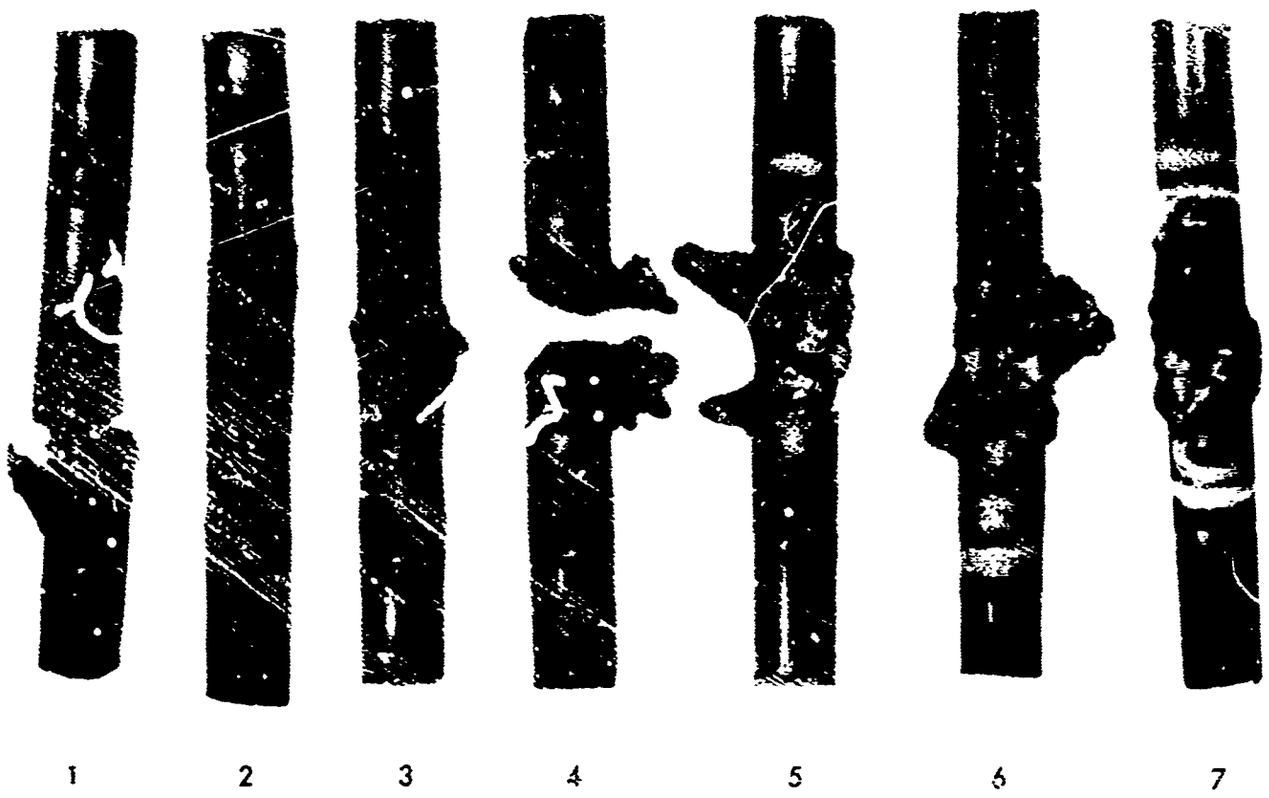

Figure 2. Appearance of 8Ta-55Hf-37C Microcomposites After Exposure to Al_2O_3 Seeded Plasma Jet Tests. The Specimen Number Identity Can Be Correlated with Test Conditions Given In Table 1.

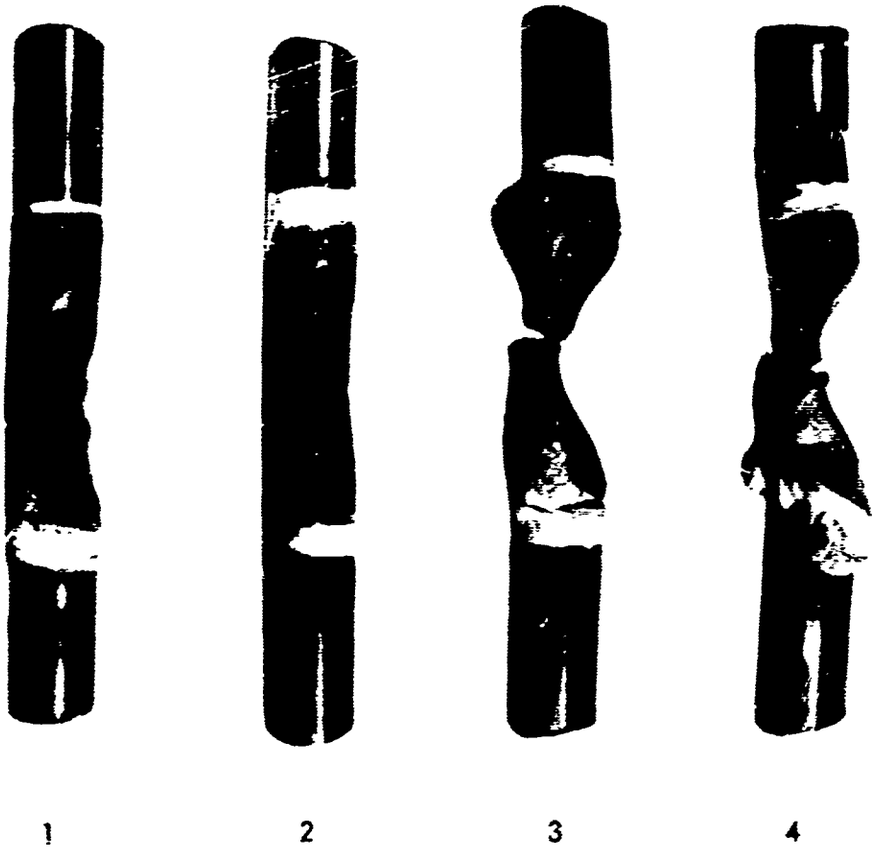

Figure 3. Appearance of 6Ta-5Hf-3C Microcomposites After Exposure to Al_2O_3 Seeded Plasma Jet Tests. The Specimen Number Can Be Correlated with Test Conditions Listed in Table I

TABLE I

Plasma Jet Impingement Data, Al_2O_3 Seeded

Specimen No.	Preheat Temperature °F	Test Temperature °F	Recession Rate inches/min.
8Ta-55Hf-37C Composition			
3	4050	5400	0.035
4	3720	5450	0.096
5	3000	5550	0.074
6	2300	5400	0.038
7	None	5050	0.018
8Ta-54Hf-38C Composition			
1	1500	5800	0.010
2	None	5500	0.030
3	1500	5400	0.060
4	1500	5600	0.040

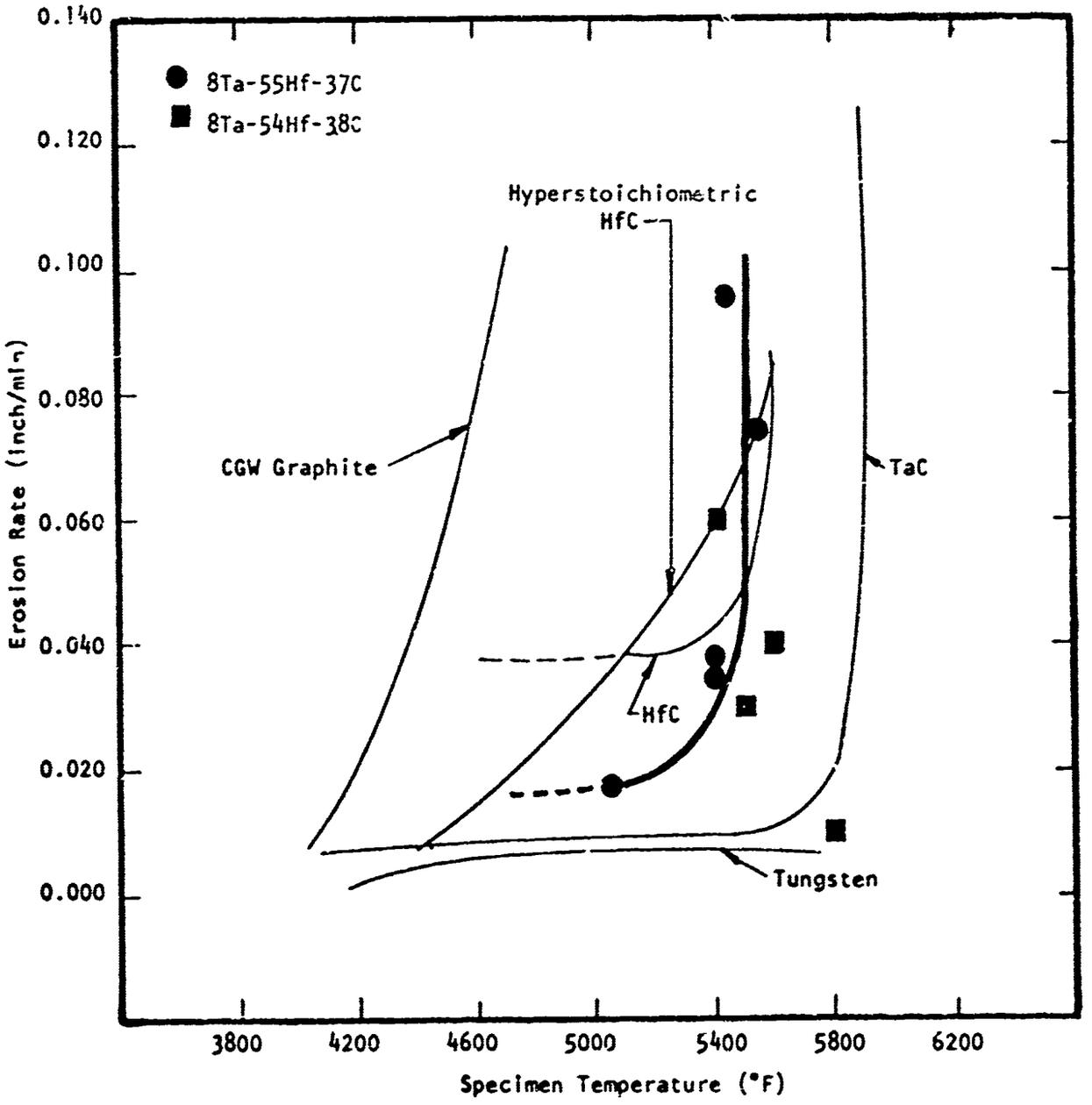

Figure 4. Erosion Rates of Ta-Hf-C Microcomposites Compared to Various Nozzle Materials, Plasma Jet Impingement Tests, Alumina Seeded, 0.5 lbs/hr.

TABLE 2

Test Conditions for the Alumina-Microcomposite Carbide

Static Reactivity Tests

Specimen No.	Composition	Test Temperature °F	Test Duration Minutes
1	8Ta-54Hf-38C	4600	3.0
2	8Ta-54Hf-38C	5100	3.0
3	8Ta-54Hf-38C	4800	2.2
4	8Ta-55Hf-37C	5300	3.0

Disposition of Microcomposite Specimens Received

	8Ta-55Hf-37C	8Ta-54Hf-38C
Plasma Jet Test	7	4
Metallography (as-received)	1	1
Static Reactivity	1	3
Broken Before Testing	1	2
Totals	10	10

4600°F
3 min.

5100°F
3 min.

4800°F
2.2 min.

Figure 5. Appearance of 8Ta-54Hf-38C Microcomposites After Exposure to Al_2O_3 in the Static Reactivity Tests

In all tests, the alumina readily wet the microcomposite surface and flowed out of the cavity covering the entire heated surface of the specimen. After testing, the specimens were evaluated for the extent and mechanism of chemical reaction with the alumina by use of metallography, electron microprobe analysis, and x-ray diffraction. The results of these examinations are discussed lated in this report.

Hypereutectic TaC-C Composites

Plasma-jet impingement tests - The data derived from the plasma jet impingement tests of the hypereutectic TaC-C carbide composites are tabulated in Table 3. Specimens of the third group, after testing, are presented in Figure 6. A cycle time of 3 minutes at temperature was maintained except for specimens Nos. 3 and 6, Figure 6. Specimen No. 3 eroded completely through after 2 minutes. The test of specimen No. 6 was aborted after 30 seconds by failure of the plasma jet nozzle which resulted in thermal stress failure of the specimen. The fourth group of specimens shown in Figure 7 were all tested with a 3 minute cycle time.

The erosion rate of both carbide materials is plotted as a function of test temperature in Figure 8. The erosion rates of other refractory nozzle materials as well as the microcomposites tested previously are included in the graph of Figure 8 for comparison.

The erosion resistance of both of the hypereutectic carbide specimens to the alumina seeded plasma flame are comparable and difficult to separate. The data are also characterized by a large degree of scatter. The erosion resistance as a function of temperature is lower than that of the Ta-Hf-C microcomposite materials tested in this program. A threshold temperature such as was found to exist for the microcomposite materials was not sharply defined for the hypereutectic carbides.

Static reactivity tests - The static reactivity tests were performed under the same conditions as were used in testing the microcomposite materials. The conditions of testing the TaC-C composites are tebulated in Table 4.

In all tests, the alumina readily wet the carbide surface and flowed out of the cavity covering the entire heated surface of the specimen. Visual examination of the specimens after the test showed no evidence of gross damage, and heated surfaces were bright and clean.

TABLE 3

Plasma Jet Impingement Data, Al_2O_3 Seeded

3rd Group of Carbide Composites

Identification No.	Aerojet Specimen No.	Preheat Temp. °F	Test Temp. °F	Recession Rate in/min.
1	463-b	None	4650	.023
2	463-d	1500	4760	.038
3	463-e	1925	5030	.125
4	463-j	None	5090	.014
5	463-c	1600	5250	.083
6	463-h	3100	5610	.116

4th Group of Carbide Composites

1	487-6	None	4550	.004
2	487-5	3000	4870	.083
3	487-4	None	4920	.026
4	487-2	None	5200	.018
5	487-3	1500	5300	.057
6	487-1	None	5640	.021

Figure 6. Appearance of the 3rd Group of Carbide Composites After Exposure to Al_2O_3 Seeded Plasma Jet Tests.

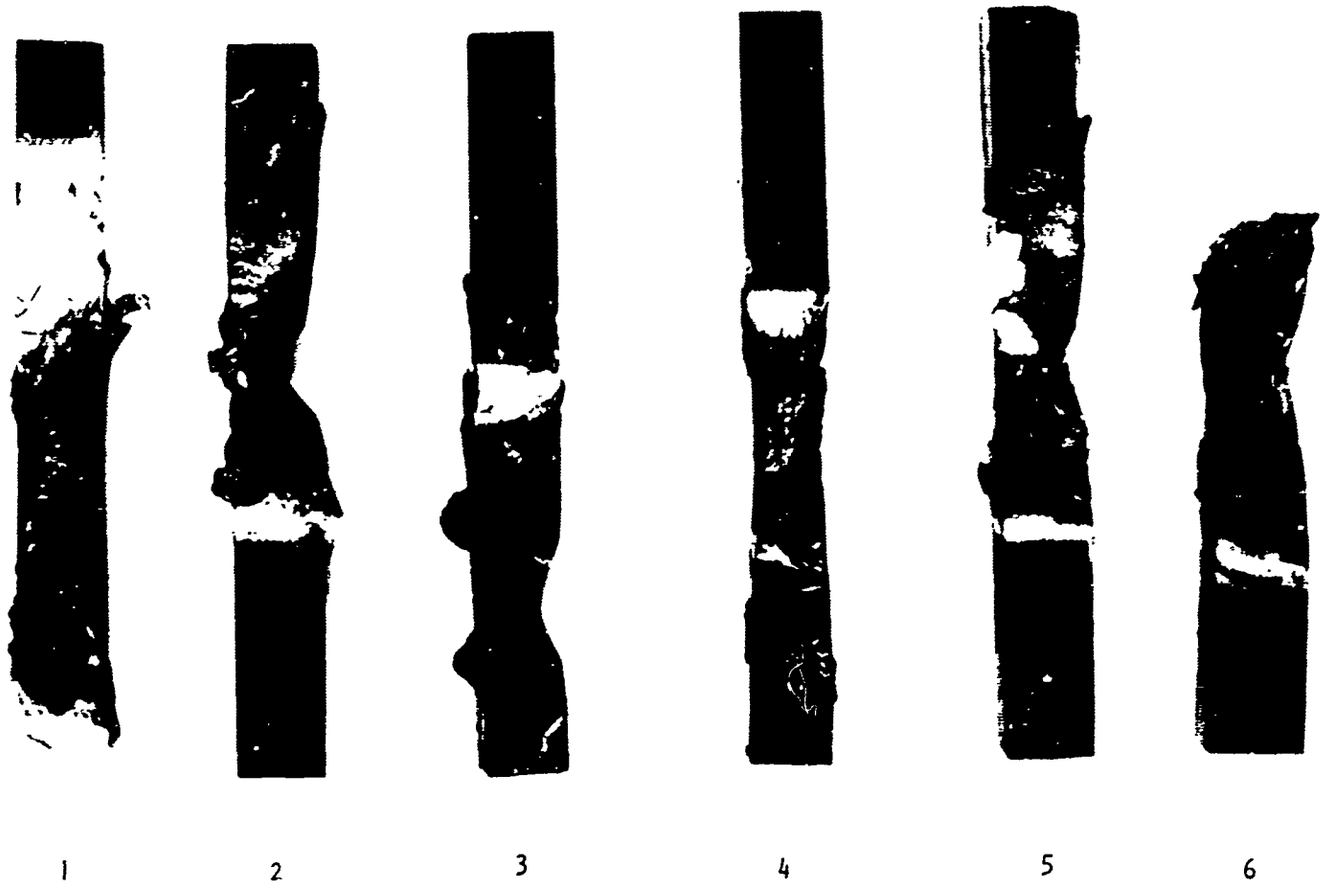

Figure 7. Appearance of the 4th Group of Carbide Composites After Exposure to Al_2O_3 Seeded Plasma Jet Tests

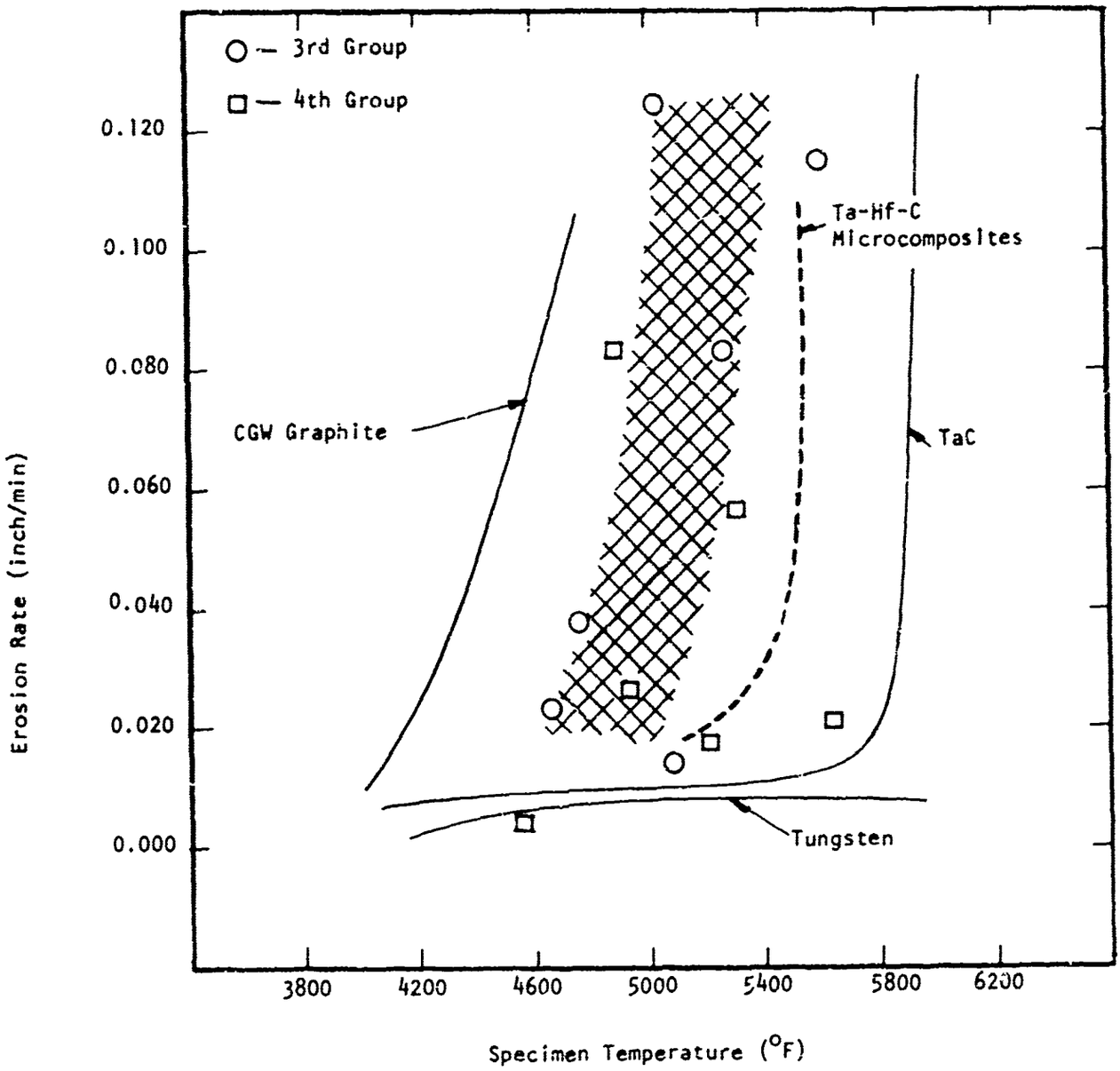

Figure 8. Erosion Rates of Hypereutectic TaC-C Carbides Compared to Various Nozzle Materials During Impingement with a Plasma Jet Seeded with Alumina at 0.5 lbs./hr.

TABLE 4

Static Reactivity (Sessile Drop) Test-Al_2O_3

3rd Group of Carbide Composites

Identification No.	Aerojet Specimen No.	Test Temperature °F	Test Duration Minutes
1	463-f	4650	3
2	462-h	4800	3
3	462-c	4850	3
4	462-j	5300	1.5

4th Group of Carbide Composites

1	488-1	Broken before testing	
2	488-2	4750	3
3	488-4	Broken before testing	
4	488-3	Broken before testing	

Metallurgical Analysis of Specimens

After the carbide specimens were subjected to either the plasma jet impingement test or the static reactivity test, selected specimens were examined by various metallurgical techniques to evaluate the nature and mechanism of chemical reactivity with the alumina. This analysis included metallography, electron microprobe analysis, and x-ray diffraction analysis.

Metallography - Typical microstructures of the microcomposite materials both as-received and after plasma jet testing are shown in Figures 9 and 10. The photomicrograph of Figure 10 indicates considerable penetration of alumina into the specimen. The typical reaction was an intergranular attack. This is illustrated in Figure 11, a sessile drop specimen of the 8Ta-54Hf-38C composition heated to 4600°F. In this specimen, attack by the alumina penetrated to a depth of 60 mils below the surface of the specimen. No evidence of general melting was found on this specimen. This degree of attack and resulting microstructure is typical of all the microcomposite specimens tested (including the 8Ta-55Hf-37C specimens). A the higher temperatures, it might be expected that attack would be more severe. However, the wetting of the entire specimen surface by the alumina at over 5000°F proceeded so rapidly that the alumina rapidly left the specimen cavity and was therefore unable to support localized attack.

The static reactivity specimen tested at 4800°F underwent more severe reaction and showed indications that significant molten material had been present at the test temperature. It is presumed that the molten phase was a eutectic formed by the carbode composite and the alumina. Metallographic examination of this specimen after testing, however, showed a microstructure similar to that of the other specimens, as shown in Figure 11. One explanation of the accelerated reaction at 4800°F is that, up to this temperature, the rate of chemical attack increased faster than the ability of the alumina to escape from the cavity by its increased wettability. Therefore, the alumina remained concentrated in one area of the specimen to support the localized reaction.

The as-received hypereutectic TaC-C composites were characterized by a variety of microstructures as shown in Figure 12. The predominant microstructure, however, is the carbide matrix with finely distributed graphite and containing relatively massive graphite plates illustrated in Figure 12b. The microstructure of typical specimens subjected to the Al_2O_3 seeded plasma jet test are presented in Figure 13. In contrast to the microcomposites, the attack on the hypereutectic carbides is not intergranular but proceeds along the paths occupied by the massive graphite plates. As will be shown later, the single phase area shown in Figure 13a is tantalum oxide formed in the location presumable formerly occupied by a graphite flake.

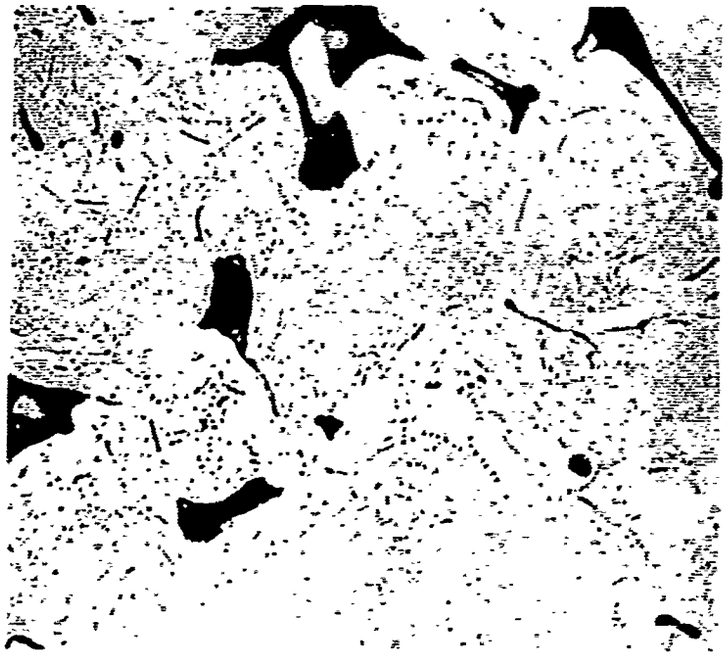

Figure 9. Microstructure of the as-received microcomposite. 500X

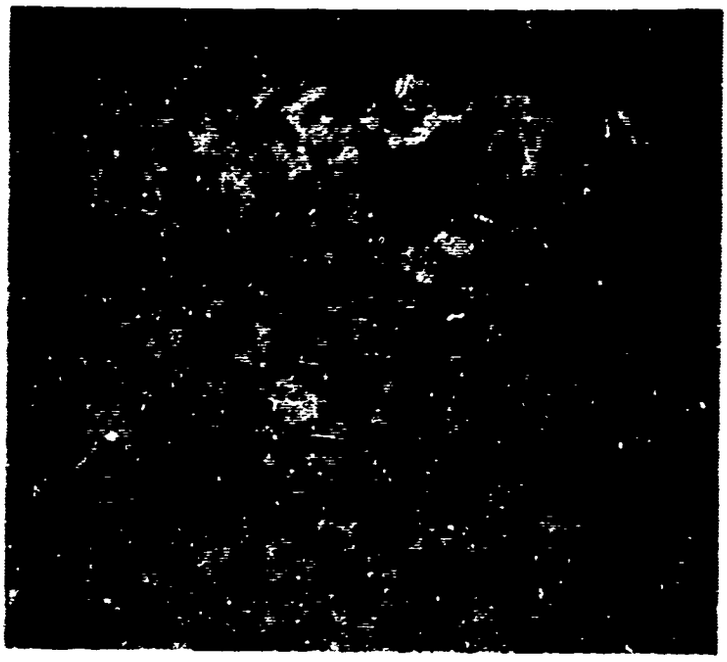

Figure 10. Microcomposite material after the alumina seeded plasma jet test at 5600°F. 250X

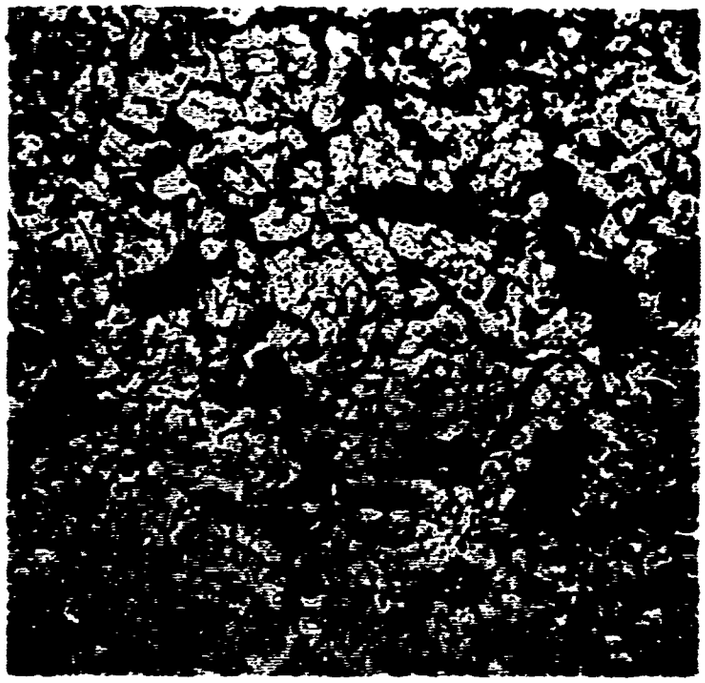

500X

Figure 11. Microstructure of the 8Ta-54Hf-38C Microcomposite After a 3 Minute Exposure at 4600°F in Contact With Al_2O_3.

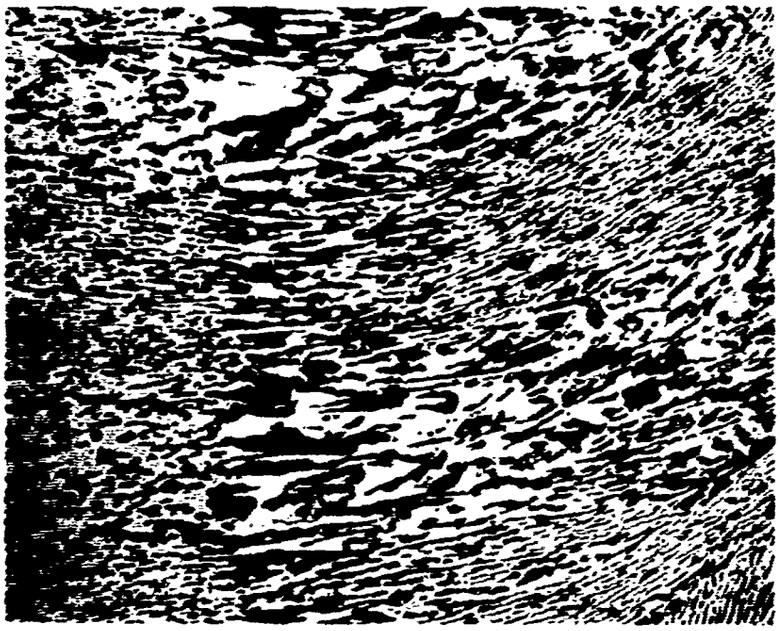

(a) 75X

(b) 75X

Figure 12. Microstructure of As-Received TaC-C Hypereutectic Composite. Aerojet Specimen No. 462J

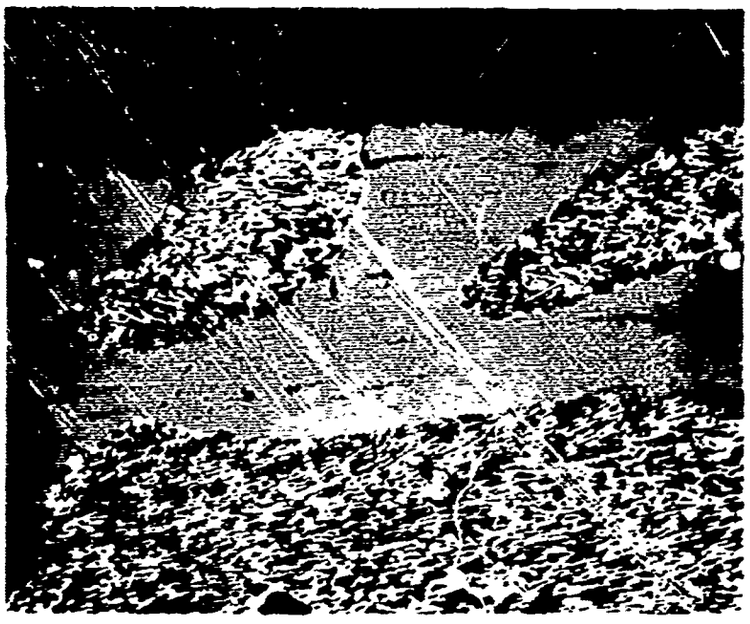

(a) Aerojet Specimen No. 463b
Plasma Jet Tested for 3 Minutes at 4650°F

250X

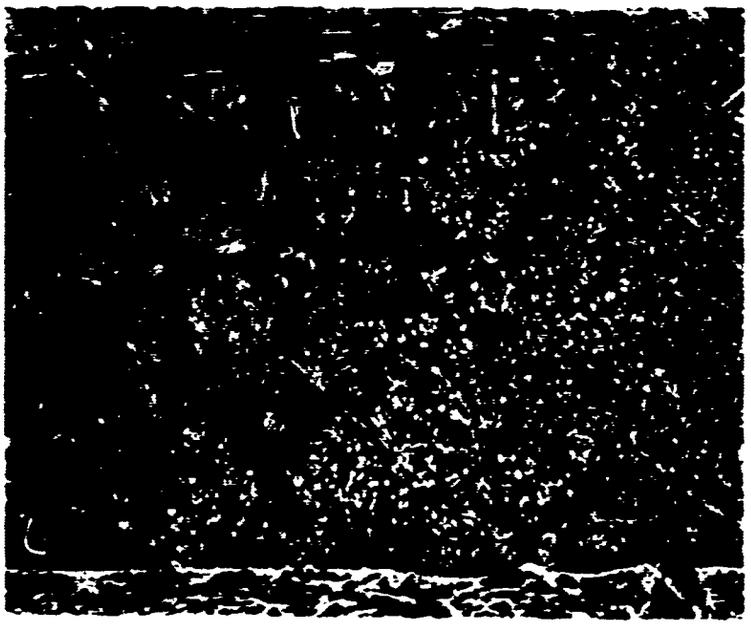

(b) Aerojet Specimen No. 487-1
Plasma Jet Tested for 3 Minutes at 5640°F

250X

Figure 13. Hypereutectic TaC-C Composites after the Al_2O_3 Seeded Plasma Jet Test. For Aid in Interpreting Microstructure, See Microprobe Analysis in Figure 17.

Electron microprobe analysis - Electron microprobe analyses were performed on these specimens in order to help define the mechanism of attack on the carbide composite by the alumina. Electron microprobe photos of the reacted area of the 8Ta-54Hf-38C microcomposite, specimen No. 4 - Table I, after plasma jet testing at 5600°F, are shown in Figure 14. The photographs show that the attack is proceeding primarily at the expense of the hafnium (by the correspondence of the Hf and the Al x-ray patterns). This same mechanism of attack is indicated in the static reactivity test specimens. A typical set of results (for specimen No. 1, 8Ta-54Hf-38C microcomposite, 4600°F exposure) are shown in Figure 15. These photographs indicate the following:

1. Segragation of Ta is taking place

2. Localized areas of aluminum are evident with some relation to the oxygen distribution (indicating Al_2O_3)

3. A possible indication of attack of the HfC by Al_2O_3 based on the similar distributions of the HF, C, and oxygen patterns

The results of the specimen tested at 5100°F show these same trends, and in a less subtle manner. These results, presented in the series of photographs in Figure 16, indicate the following:

1. Segragation of the Hf and Ta: the high intensity (light) areas in the Ta and the Hf images are not coincident.

2. Presence of oxides of Al and Hf: areas of high oxygen and aluminum roughly corresponding to areas rich in hafnium

3. Relatively uniform carbon distribution but somewhat higher in areas of high oxygen indicating chemical attache by Al_2O_3, is on HfC rather than on metallic constituents.

Typical sets of results of the electron microprobe analysis of the hypereutectic carbides are shown in Figures 17 and 18. The analysis of specimen 463b - Table 3 shown in Figure 17 was performed at the point of greatest erosion within the body of the specimen. The analysis shown in Figure 18, was performed on the same specimen but at the midpoint within the reaction product which had built up on the O.D. during the plasma jet test. The photograph of Figure 17 shows a wide distribution of Ta and O_2 with a faint but discernable pattern, almost no Al, and a distribution pattern of C. The coincident patterns of Ta and O_2 and the low level of C in the single phase region, coupled with the virtual absence of Al, show the single phase region to be composed of tantalum oxide.

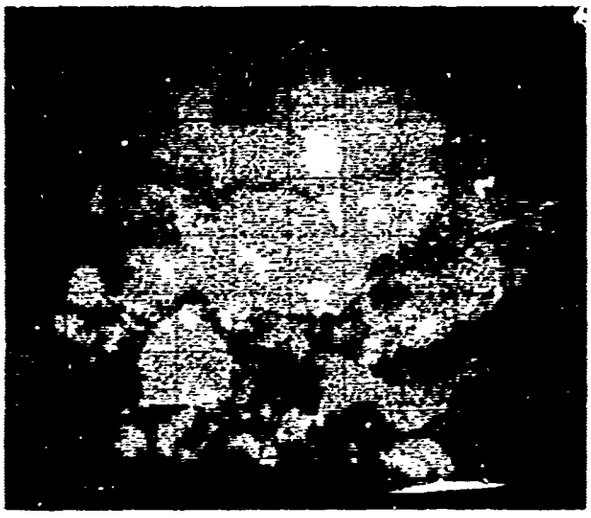

Hf X-Rays 400X

Ta X-Rays 400X

Al X-Rays 400X

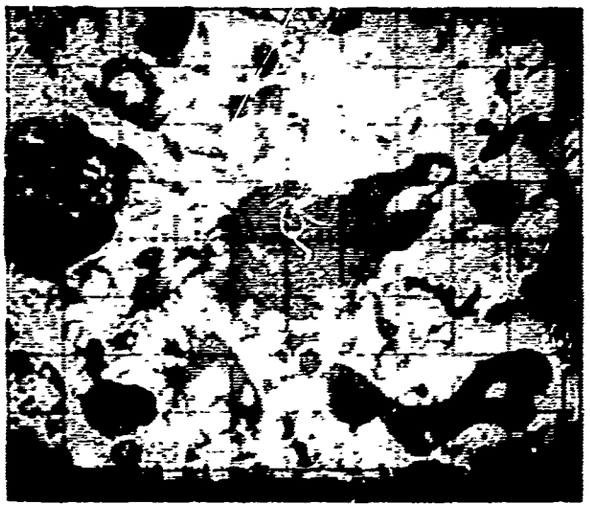

Sample Current 400X

Figure 14. Electron Microprobe Photographs of the Microcomposite Material After the Alumina Seeded Plasma Jet Test at 5600°F

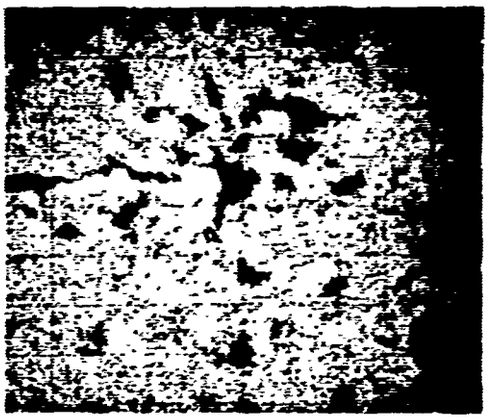

Ta X-rays 400X

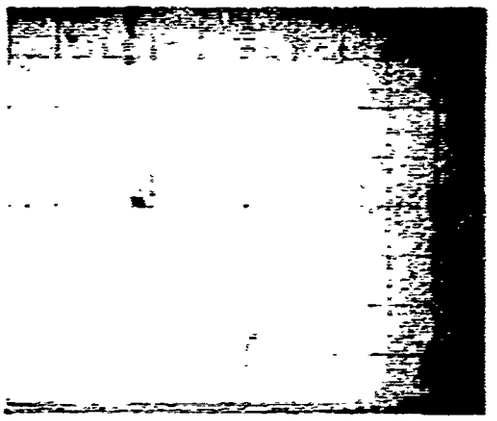

Hf X-rays 400X

C X-rays 400X

O X-rays 400X

Al X-rays 400X

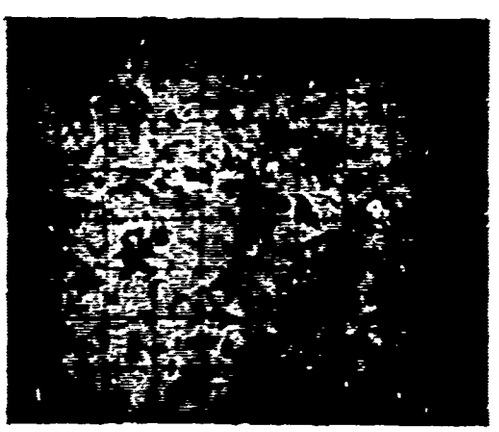

Sample Current 400X

Figure 15. Electron Microprobe Photographs of the 8Ta-5Hf-3C Microcomposite after Static Reactivity Testing at 4600°F in Contact with Al_2O_3

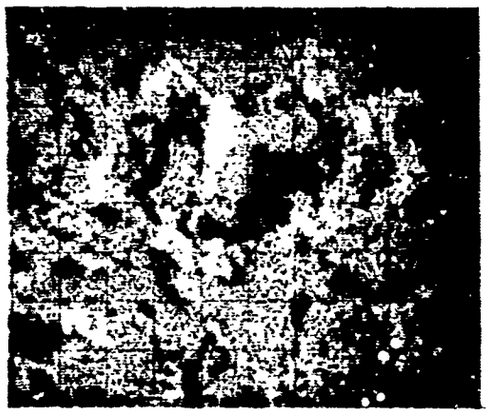

Ta X-rays 400X

Hf X-rays 400X

C X-rays 400X

O X-rays 400X

Al X-rays 400X

Sample Current 400X

Figure 16. Electron Microprobe Photographs of the 8Ta-54Hf-38C Microcomposites after Static Reactivity Testing at 5100°F in Contact with Al_2O_3

Secondary Current 300X

Photomicrograph 250X

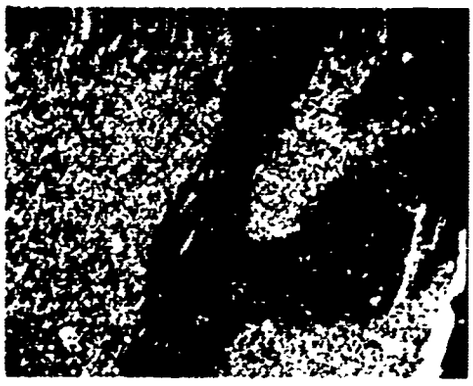

C X-Rays 300X

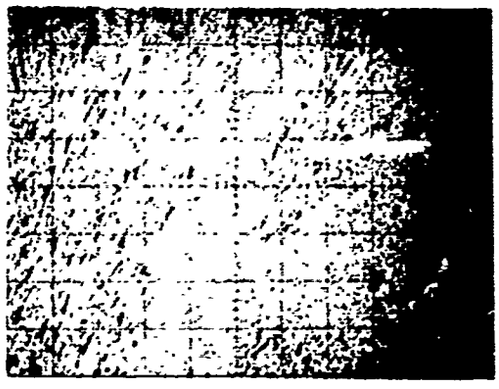

Ta X-Rays 300X

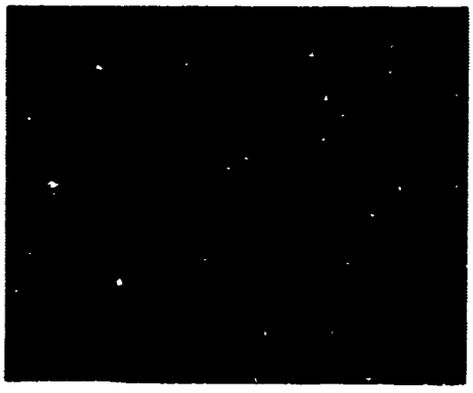

Al X-Rays 300X

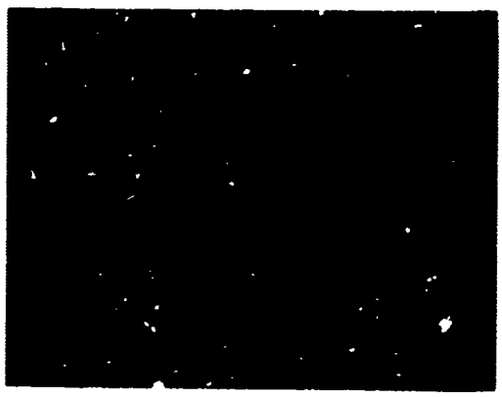

O_2 X-Rays 300X

Figure 17. Electron Microprobe Photographs of the Reacted Zone within the TaC-C Composite, Specimen 463b - Table 3, after The Alumina Seeded Plasma Jet Test at 4650°F/

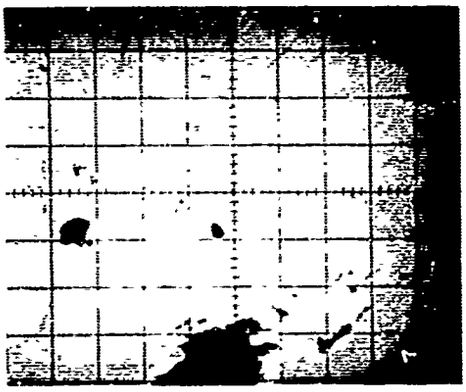

Secondary Current 300X

Al X-Rays 300X

Ta X-Rays 300X

C X-Rays 300X

O_2 X-Rays 300X

Figure 18. Electron Microprobe Photographs of the Area within The Build Up Reaction Product of the TaC-C Composite Specimen 463b - Table 3, After the Alumina Seeded Plasma Jet Test at 4650°F

In the analysis of the reaction product (Figure 18), the uniform distribution of Ta and O_2 and the low level of C and Al indications, show the reaction product to be tantalum oxide. A qualitative analysis of the reaction product (2 ϕ scan) made with the electron microprobe in the same area shown in Figure 18, revealed the majo. element to be Ta with a trace of Al.

The initial stages of the reaction are presented in Figure 19, an analysis performed on the static reactivity specimen No. 488-2 - Table 3 after a 3 minute exposure at 4750°F in the sessile drop test. The photographs show a high concentration of C in the alumina build up and also the penetration of alumina along the channel once occupied by a graphite plate.

X-ray diffraction - X-ray diffraction studies were made on the as-received material and on the static reactivity tested material. Measurements were made using a Norelco Diffractometer with CuKα radiation and Ni filter.

The as-received microcomposite materials were primarily FCC λ (HfTa)C with lattice parameter of 4.606 A. The x-ray diffraction pattern also showed a strong line for metallic Hf (d spacing (101) of 2.42 A). The static reactivity tested material showed that two distinct carbides are present; both are FCC λ (HfTa)C with lattice parameters of 4.591 A and 4.580 A. This material also yielded a strong line for HCP Hf with a (101) d spacing of 2.40 A. This indicates some dissolved Ta in the metallic Hf. The one apparent explanation that is consistant with the phase diagram data is that Hf is selectively removed from the matrix carbide on exposure, thus causing a localized lattice parameter reduction.

X-ray diffraction studies were also made on typical specimens of the plasma jet and sessile drop hypereutectic carbide materials. The x-ray diffraction patterns indicated the major constituent to be TaC with varying (slight to appreciable) quantities of the high temperature form of Ta_2O_5. Indications of an unknown compound (which could be a non-stoichiometric tantalum oxide) were also found. The presence of Al_2O_3 was not detected by the x-ray diffraction analysis on any of the samples tested.

Secondary Current 300X

Microstructure 250X

C X-Rays 300X

Ta X-Rays 300X

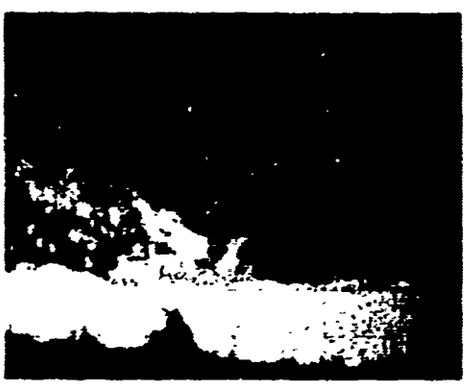

Al X-Rays 300X

O_2 X-Rays 300X

Figure 19. Electron Microprobe Photographs of the TaC-C Composite, (Specimen No 488-2 - Table 4), after Static Reactivity Testing at 4750°F

DISCUSSION OF RESULTS

The plasma jet impingement tests and the static reactivity tests performed in this program show that significant differences exist in the response to these tests by the two major types - micro-composites and hypereutectic TaC-C - of carbide materials evaluated. As shown in Figure 8, both types of material show erosion behavior in the general range defined by previous tests of other graphitic and carbide-type materials. Figure 8 also shows that the hypereutectic material can be expected to experience a given erosion rate at several hundred degrees (°F) lower temperature than the microcomposites.

There was no significant difference in behavior noted for the various material compositions within the two main classes of carbide materials. The compositional differences between the two microcomposites was slight. It should be noted that the compositions of the hypereutectic carbides were not supplied to TRW. The difference between the two sets of hypereutectic carbide samples supposedly was a TaC coating on the one set. No coating was evident, however, so it is thought these two sets of specimens may have been essentially identical.

In addition to the actual difference in the erosion rates between the microcomposite and the hypereutectic carbides, the more significant difference is in the mechanism of attack. Understanding the mechanism of reaction is the first step in being able to extrapolate the data to actual rocket firing conditions and in developing realistic approaches for improved materials. The aspects of the reaction of Al_2O_3 with these types of carbides as brought to light in this program are summarized below:

Microcomposites

The mechanism responsible for the accelerated erosion rate of the microcomposite carbides appears to be a eutectic reaction between the liquid alumina particles and hafnium in the microcomposite. The electron microprobe analysis shows that the attack is proceeding primarily at the expense of the hafnium. The reaction between HfC and liquid Al_2O_3 has been found to be exothermic in previous tests in this laboratory which would explain the rapid increase in erosion above 5400°F.

The exothermic reaction would also explain the reason that pre-heat temperatures have so little influence on the final test temperature achieved by the plasma jet. As the data in Table I indicate, there is little correlation between preheat temperature and test temperature even though power input to the plasma torch was constant throughout the series of tests. The electron microprobe examination also indicates segregation of tantalum and hafnium has occurred which allows the composite material to act in a similar manner to HfC during the course of the plasma jet test.

The behavior of the microcomposite material in the static reactivity test is similar to its behavior in the plasma jet impingement test. The degradation mechanism is chemical in nature, and involves an exothermic eutectic reaction of Al_2O_3 and HfC. The reaction mechanism proceeds more rapidly in the plasma impingement test because the impinging Al_2O_3 particles provide a continuous intimate contact of the reactive components. The sweeping action of the jet also serves to remove the reacted material to permit the reaction to continue.

The temperature at which the reaction rate becomes very significant can be as low as approximately 4800°F, as was indicated by specimen No. 3, Figure 5. The relatively undamaged appearance of specimen No. 2 (5100°F exposure), Figure 5 is probably due to the fact that most of the Al_2O_3, extremely fluid at the test temperature of 5100°F, flowed out of the pocket leaving too little material at the hottest protion of the specimen to permit the reaction to become damaging.

The plasma jet impingement test demonstrated that the maximum use temperature for the microcomposite materials in contact with Al_2O_3 is below 5400°F. The static reactivity tests indicated that the useful temperature limit of these materials may be as low as 4800°F. The usefulness of these microcomposites as rocket nozzle throat insert materials in contact with Al_2O_3 at surface temperatures between 4800 and 5400°F will likely be dependent on specific conditions of use, such as gas pressure, alumina content of exhaust, and required length of the duty cycle.

Hypereutectic Carbides

The erosion of the TaC-C hypereutectic composites in the Al_2O_3 seeded plasma-jet tests results from a chemical reaction aided by mechanical erosion from the plasma jet stream. The chemical reaction probably proceeds by a reduction of alumina by carbon and the subsequent formation of tantalum oxide. The absence of Al in most of the electron microprobe photographs is due to vaporization of the Al as a metal or in the form of a carbide.

The speed of the reaction depends on the presence of liquid alumina and free carbon in sufficient quantities to sustain the reaction. The random, but not necessarily uniform, distribution of graphite plates in the hypereutectic microstructure would then account for the scatter of data points observed in the Al_2O_3 seeded plasma jet tests.

CONCLUSIONS AND PREDICTION OF FIRING BEHAVIOR

A secondary objective of the subject program is to establish the validity of the Al_2O_3 seeded plasma jet test in conjunction with the static reactivity test as a laboratory tool for evaluation of rocket nozzle throat materials. A prediction of the performance of the composite carbides in two test firings to be conducted under Contract AF04(611)-11608 are made using data derived from the laboratory tests together with an outline of the test firing conditions and an estimate of the nozzle wall temperature furnished by the Government.

The composite materials are to be test fired on the AFRPL 40-inch diameter uncured propellant test motor under the following conditions: burn time of 60 seconds; estimated motor MEOP of 700 psi; propellant aluminum content of 27%.

The thermal map provided by the government indicates a predicted temperature of 4960°F at the hottest point of the insert wall at T=5 seconds. Extrapolation of these data indicates that the throat insert wall will reach a temperature of 5400°F shortly before T=25 seconds.

The plasma jet and static reactivity test data indicates that 5400°F is the threshold temperature for the microcomposite materials. Above this temperature, the erosion rate becomes catastrophic because of a eutectic reaction between the liquid alumina and the hafnium in the microcomposite.

The threshold temperature for the TaC-C hypereutectic composites was not sharply defined by the plasma jet tests. The threshold temperature is, however, below 5400°F. Consequently, the laboratory test data indicated a greater degree of erosion for the hypereutectic composites.

The plasma jet and static reactivity test data then predict an erosion rate of 0.040 to 0.100 inches per minute for the microcomposite (8Ta-55Hf-37C and 8Ta-54Hf-38C) as a result of the test firing. The erosion rate of the hypereutectic TaC-C composites is predicted to be in the range of 0.080 to 0.120 inches per minute. By such an analysis, a 60-second firing cycle would proceed for about 25 seconds with little or no erosion (perhaps about 0.1 mil per second). The remaining 35 seconds could yield an erosion rate as high as 2 mils per second in the case of the hypereutectic carbides. The average erosion rate observed for such a 60-second test would then be expected to be in the range of about 1.2 mils per second.

The prediction is based on the assumption that the limiting factor in erosion is the chemical reactions taking place between the nozzle insert material and the liquid alumina in the exhaust gases. The complexing effects of other species in the exhaust flame have not been assessed by the plasma jet or static reactivity laboratory tests, but they may well affect the overall erosion of the nozzle throat.

Unclassified

Security Classification

DOCUMENT CONTROL DATA - R&D

(Security classification of title, body of abstract and indexing annotation must be entered when the overall report is classified)

1 ORIGINATING ACTIVITY (Corporate author) TRW inc. Materials Technology Laboratory Cleveland, Ohio 44117	2a REPORT SECURITY CLASSIFICATION Unclassified 2b GROUP

3 REPORT TITLE

Carbides for Solid Propellant Nozzle Systems

4 DESCRIPTIVE NOTES (Type of report and inclusive dates)

Final 1 October 1967 to 30 June 1968

5 AUTHOR(S) (Last name, first name, initial)

Lally, F. T.
Laverty, D. P.

6 REPORT DATE	7a TOTAL NO OF PAGES	7b NO OF REFS
1 October 1968	33	-

8a CONTRACT OR GRANT NO	9a ORIGINATOR'S REPORT NUMBER(S)
F04611-67-c-0094 b PROJECT NO 3059 c d	ER-7307 9b OTHER REPORT NO(S) (Any other numbers that may be assigned this report)

10 AVAILABILITY/LIMITATION NOTICES This document is subject to special export controls and each transmittal to foreign governments or foreign nationals may be made only with prior approval of the Air Force Rocket Propulsion Laboratory, Edwards, California.

11 SUPPLEMENTARY NOTES	12 SPONSORING MILITARY ACTIVITY
	Air Force Rocket Propulsion Laboratory Edwards, California

13 ABSTRACT The magnitude of reactivity between Al_2O_3 and carbide composite rocket nozzle throat materials was assessed by means of laboratory tests. A secondary objective of the program was to establish the validity of the laboratory tests in evaluating material performance. The program included a plasma jet test that measured mechanical and chemical erosion and a static reactivity test to separate the purely chemical effects. A prediction of the performance of the carbide composites in a test firing was made, based on the laboratory tests.

DD FORM 1 JAN 64 1473

Security Classification

Security Classification

14 KEY WORDS	LINK A		LINK B		LINK C	
	ROLE	WT	ROLE	WT	ROLE	WT

INSTRUCTIONS

1. ORIGINATING ACTIVITY: Enter the name and address of the contractor, subcontractor, grantee, Department of Defense activity or other organization *(corporate author)* issuing the report.

2a. REPORT SECURITY CLASSIFICATION: Enter the overall security classification of the report. Indicate whether "Restricted Data" is included. Marking is to be in accordance with appropriate security regulations.

2b. GROUP: Automatic downgrading is specified in DoD Directive 5200.10 and Armed Forces Industrial Manual. Enter the group number. Also, when applicable, show that optional markings have been used for Group 3 and Group 4 as authorized.

3. REPORT TITLE: Enter the complete report title in all capital letters. Titles in all cases should be unclassified. If a meaningful title cannot be selected without classification, show title classification in all capitals in parenthesis immediately following the title.

4. DESCRIPTIVE NOTES: If appropriate, enter the type of report, e.g., interim, progress, summary, annual, or final. Give the inclusive dates when a specific reporting period is covered.

5. AUTHOR(S): Enter the name(s) of author(s) as shown on or in the report. Enter last name, first name, middle initial. If military, show rank and branch of service. The name of the principal author is an absolute minimum requirement.

6. REPORT DATE: Enter the date of the report as day, month, year, or month, year. If more than one date appears on the report, use date of publication.

7a. TOTAL NUMBER OF PAGES: The total page count should follow normal pagination procedures, i.e., enter the number of pages containing information.

7b. NUMBER OF REFERENCES: Enter the total number of references cited in the report.

8a. CONTRACT OR GRANT NUMBER: If appropriate, enter the applicable number of the contract or grant under which the report was written.

8b, 8c, & 8d. PROJECT NUMBER: Enter the appropriate military department identification, such as project number, subproject number, system numbers, task number, etc.

9a. ORIGINATOR'S REPORT NUMBER(S): Enter the official report number by which the document will be identified and controlled by the originating activity. This number must be unique to this report.

9b. OTHER REPORT NUMBER(S): If the report has been assigned any other report numbers *(either by the originator or by the sponsor)*, also enter this number(s).

10. AVAILABILITY/LIMITATION NOTICES: Enter any limitations on further dissemination of the report, other than those imposed by security classification, using standard statements such as:

(1) "Qualified requesters may obtain copies of this report from DDC."

(2) "Foreign announcement and dissemination of this report by DDC is not authorized."

(3) "U. S. Government agencies may obtain copies of this report directly from DDC. Other qualified DDC users shall request through _____."

(4) "U. S. military agencies may obtain copies of this report directly from DDC. Other qualified users shall request through _____."

(5) "All distribution of this report is controlled. Qualified DDC users shall request through _____."

If the report has been furnished to the Office of Technical Services, Department of Commerce, for sale to the public, indicate this fact and enter the price, if known.

11. SUPPLEMENTARY NOTES: Use for additional explanatory notes.

12. SPONSORING MILITARY ACTIVITY: Enter the name of the departmental project office or laboratory sponsoring *(paying for)* the research and development. Include address.

13. ABSTRACT: Enter an abstract giving a brief and factual summary of the document indicative of the report, even though it may also appear elsewhere in the body of the technical report. If additional space is required, a continuation sheet shall be attached.

It is highly desirable that the abstract of classified reports be unclassified. Each paragraph of the abstract shall end with an indication of the military security classification of the information in the paragraph, represented as *(TS), (S), (C), or (U)*

There is no limitation on the length of the abstract. However, the suggested length is from 150 to 225 words.

14. KEY WORDS: Key words are technically meaningful terms or short phrases that characterize a report and may be used as index entries for cataloging the report. Key words must be selected so that no security classification is required. Identifiers, such as equipment model designation, trade name, military project code name, geographic location, may be used as key words but will be followed by an indication of technical context. The assignment of links, rules, and weights is optional.

Security Classification